An Integrated Coupled Inductor and Switched-Capacitor Based High Gain DC/DC Converter for Closed Loop Control of DC Motor

D.Madhu, D.Krishna Chaitanya, S.M.Shariff

Abstract -The voltage gain of Conventional boost converter is limited due to the high current ripple, high voltage stress across active switch and diode, and low efficiency associated with large duty ratio operation. High voltage gain is required in applications, such as the renewable energy power systems with low input voltage. A high step-up voltage gain active-network converter with switched capacitor technique is proposed in this project. The proposed converter can achieve high voltage gain without extremely high duty ratio. In addition, the voltage stress of the active switches and output diodes is low. Therefore, low voltage components can be adopted to reduce the conduction loss and cost. The operating principle and steady-state analysis are discussed in detail. Based on the concept of switched-inductor and switched- capacitor, this project proposes a novel switched-capacitor-based active-network converter (SC-ANC) for high step-up con- version, which has the following advantages: high voltage- conversion ratio, low voltage stress across switches and diodes, and self-voltage balancing across the output capacitors. The operating principle and steady-state analysis are discussed in detail. The simulation results are given to verify the analysis and advantages of the proposed converter

Index Terms— Coupled inductor, dc/dc converters, high step-up, switched capacitor, DC Motor

1 INTRODUCTION

THIS DC-DC converter converts directly from dc todc and is simply known as a DC converter. A dc converter can be considered as dc equivalent to an ac transformer witha continuously variable turn's ratio [1]. Like a transformer, it can be used to step down or step up a dc voltage source. Dc converters are widely used for traction motorcontrol in electric automobiles, trolley cars, marine hoists and mine haulers [2]. They provide smooth acceleration control,high efficiency and fast dynamic response. Dc converters can be used in regenerative braking of dc motors to returnenergy back into the supply and this feature results in energy savings for transportation systems with frequent stops [3-5]. Dc converters are used in dc voltage regulators; and also used in conjunction with an inductor to generate a dc current source, especially for the current source inverter [6].

A boost converter is generally used and it hasseveral advantages such as simple structure, continuous input current, and clamped switch voltage stress to the output voltage [7]. However, it is very difficult to satisfy both high voltage conversion ratio and high efficiency at once. This is primarily due to the parasitic resistances, whichcause serious degradation in the step-up ratio and efficiency as the operating duty increases [8]. Moreover, in high outputsevere reverse recovery problem and it requires a snubber.

As a result, a general boost converter would not be acceptable for high step-up applications. To overcome thislimitation, various types of step-up converters, utilizing thevoltage conversion ability of a transformer, can be adopted [9].

In order to provide such a large step-up/step-downvoltage gain, the non-isolation converters would have to work with extreme duty ratios: in the case of boost-typeconverters, a large duty ratio would be necessary, but this is not possible due to the latch-up condition [10]. Moreover, theshort conduction time of the rectifier switch determines a short pulse current with high amplitude flowing through it, and thus a severe rectifier-reverse-recovery problem.

Some transformer-based converters like forward, push–pull or flyback converters can achieve high step-up voltage gain by adjusting the turn ratio of the transformer [11]. However, the leakage inductor of the transformer will cause serious problems such as voltage spike on the main switch and high power dissipation [12]. In order to improve the conversion efficiency and obtain high step-up voltage gain, many converter structures have been presented. Switched capacitor and voltage lift techniques have been used widely to achieve high step-up voltage gain. However, in these structures, high charging currents will flow through the main switch and increase the conduction losses.

Coupled-inductor-based converters can also achieve high step-up voltage gain by adjusting the turn ratios. However, the energy stored in the leakage inductor causes a voltage spike on the main switch and deteriorates the conversion efficiency [13]. To overcome this problem,

coupled-inductor-based converters with an active-clamp circuit have been presented. Some high step-up converters with two-switch and single-switch are introduced in the recent published literatures. However, the conversion ratio is not large enough.

This paper presents a novel high step-up dc/dc converter for DC Motor. The suggested structure consists of a coupled inductor and two voltage multiplier cells in order to

obtain high-step-up voltage gain. In addition, a capacitor is charged during the switch-off period using the energy stored in the coupled inductor, which increases the voltage transfer gain. The energy stored in the leakage inductance is recycled with the use of a passive clamp circuit. The voltage stress on the main power switch is also reduced in the proposed topology. Therefore, a main power switch with low resistance RDS (ON) can be used to reduce the conduction losses. The operation principle and the steady-state analyses are discussed thoroughly.

2. OPERATING PRINCIPLE OF THE HIGH GAIN CONVERTER

The circuit configuration of the proposed converter is shown in Fig.1. The proposed converter comprises a dc input voltage (V_I), active power switch (S), coupled inductor, four diodes, and four capacitors. Capacitor C_1 and diode D_1 are employed as clamp circuit respectively. The capacitor C_3 is employed as the capacitor of the extended voltage multiplier cell. The capacitor C_2 and diode D_2 are the circuit elements of the voltage multiplier which increase the voltage of clamping capacitor C_1. The coupled inductor is modeled as an ideal transformer with a turn ratio N (NP/NS), a magnetizing inductor L_m and leakage inductor L_k.

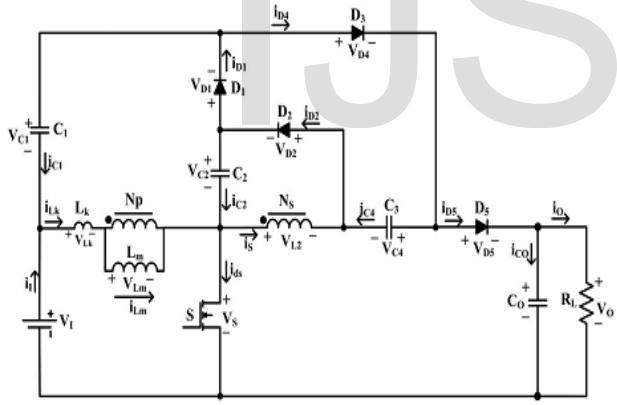

Fig.1 Circuit configuration of the presented high-step-up converter.

In order to simplify the circuit analysis of the converter, some assumptions are considered as follows:

1) All Capacitors are sufficiently large; therefore V_{C1}, V_{C2}, V_{C3}, and V_O are considered to be constant during one switching period;

2) All components are ideal but the leakage inductance of the coupled inductor is considered

According to the aforementioned assumptions, the continuous conduction mode (CCM) period. The current flow path of the proposed converter for each stage operation of the proposed converter includes five intervals in one switching is depicted in Fig.2. Some typical waveforms under CCM operation are illustrated in Fig.3. The operating stages are explained as follows.

1) Stage I [$t_0 < t < t_1$ see Fig.2 (a)]: In this stage, switch S is turned ON. Also, diodes D_2 and D_4 are turned ON and diodes D_1 and D_3 are turned OFF. The dc source (V_I) magnetizes Lm through S. The secondary-side of the coupled inductor is in parallel with capacitor C_2 using diode D_2. As the current of the leakage inductor L_k increases linearly, the secondary side current of the coupled inductor (i_s) decreases linearly. The required energy of load (R_L) is supplied by the output capacitor C_O. This interval ends when the secondary-side current of the coupled inductor becomes zero at $t = t_1$.

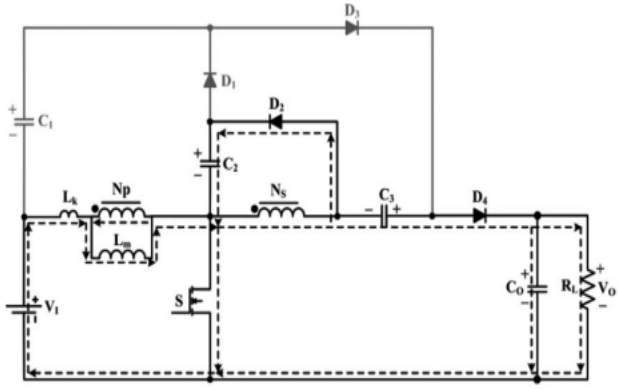

(a)

2)

3)

4) Stage II [$t_1 < t < t_2$ see Fig.2 (b)]: In this stage, switch S and diode D_3 are turned ON and diodes D_1, D_2, and D_4 are turned OFF. The dc source V_I magnetizes L_m through switch S. So, the current of the leakage inductor L_k and magnetizing inductor L_m increase linearly. The capacitor C_3 is charged by dc source V_I, clamp capacitor and the secondary-side of the coupled inductor. Output capacitor C_O supplies the demanded energy of the load R_L. This interval ends when switch (S) is turned OFF at $t = t_2$.

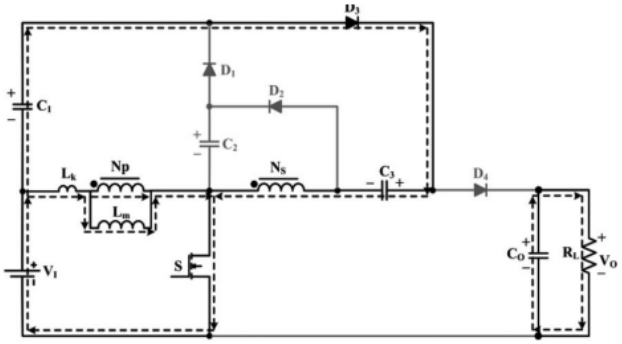

(b)

3)Stage III [$t_2 < t < t_3$ see Fig.2 (c)]: In this stage, switch S is turned OFF. Diodes D_1 and D_3 are turned ON and diodes D_2 and D_4 are turned OFF. The clamp capacitor C_1 is charged by the stored energy in capacitor C_2 and the energies of leakage inductor L_k and magnetizing inductor L_m. The currents of the secondary-side of the coupled induc-

tor (i_S) and the leakage inductor are increased and decreased, respectively. The capacitor C_3 is still charged through D_3. Output capacitor C_O supplies the energy to load R_L. This interval ends when i_{Lk} is equal to i_{Lm} at $t = t_3$.

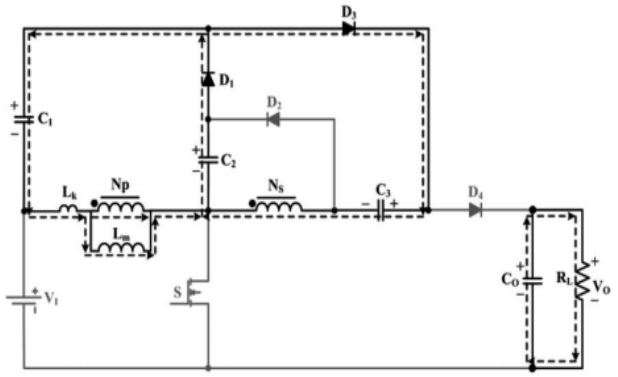

(c)

4) Stage IV [$t_3 < t < t_4$ see Fig.2 (d)]: In this stage, S is turned OFF. Diodes D_1 and D_4 are turned ON and diodes D_2 and D_3 are turned OFF. The clamp capacitor C_1 is charged by the capacitor C_2 and the energies of leakage inductor L_k and magnetizing inductor L_m. The currents of the leakage inductor L_k and magnetizing inductor L_m decrease linearly. Also, a part of the energy stored in L_m is transferred to the secondary side of the coupled inductor. The dc source V_I, capacitor C_3 and both sides of the coupled inductor charge output capacitor and provide energy to the load R_L. This interval ends when diode D_1 is turned OFF at $t = t_4$.

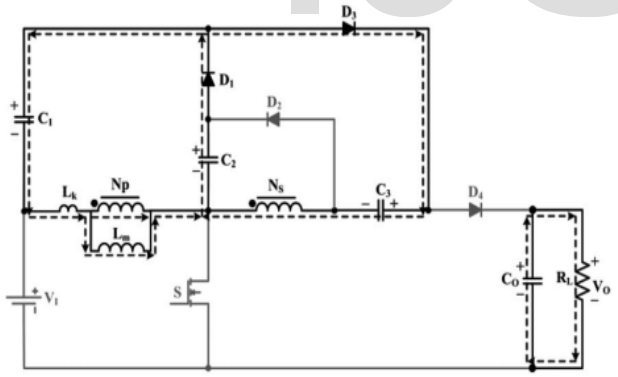

(d)

5)Stage V [$t_4 < t < t_5$ see Fig.2 (e)]: In this stage, S is turned OFF. Diodes D_2 and D_4 are turned ON and diodes D_1 and D_3 are turned OFF. The currents of the leakage inductor L_k and magnetizing inductor Lm decrease linearly. Apart of stored energy in L_m is transferred to the secondary side of the coupled inductor in order to charge the capacitor C_2 through diode D_2. In this interval the dc input voltage V_I and stored energy in the capacitor C_3 and inductances of both sides of the coupled inductor charge the output capacitor Co and provide the demand energy of the load R_L. This interval ends when switch S is turned ON at $t = t_5$.

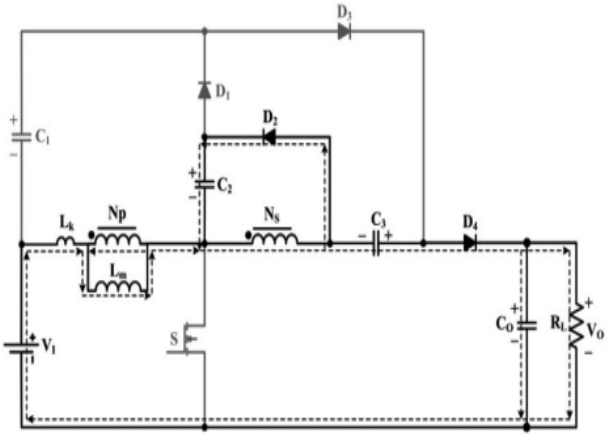

(e)

Fig.2. Current-flow path of operating modes during one switching period at CCM operation. (a) Mode I. (b) Mode II. (c) Mode III. (d) Mode IV. (e) Mode V.

3. STEADY-STATE ANALYSIS OF THE PROPOSED CONVERTER

A. CCM Operation

To simplify the steady-state analysis, only stages II, IV, and V are considered since these stages are sufficiently large in comparison with stages I and III. During stage II, Lk and Lm are charged by dc source V_I. Therefore, the following equation can be written according to Fig.2 (b):

$$V_{L_m} = kV_I \tag{1}$$

Where k is the coupling coefficient of coupled inductor, which equals to $L_m/(L_m + L_k)$. Capacitor C_3 is charged by clamp capacitor C_1, dc source (V_I), and the secondary-side of thecoupled inductor. The voltage across the capacitor C_3 can be expressed by

$$V_{C3} = V_{C1} + (kn + 1)V_I \tag{2}$$

Where n is the turn ratio of coupled inductor which is equal to N_S/N_P. As shown in Fig.2 (d), during stage IV, L_k and L_m demagnetize to the clamp capacitor C_1 with the help of capacitor C_2.

Hence, the voltage across Lm can be written as

$$V_{L_m} = k\left(V_{C2} - V_{C1}\right) \tag{3}$$

Also, the output voltage can be formulated based on Fig.2 (d)

$$V_O = V_I + V_{C3} + (kn+1)(V_{C1} - V_{C2}) \tag{4}$$

According to Fig.2 (e), in the time interval of stage V, the voltage across L_m can be expressed by

$$V_{L_m} = \frac{-V_{C2}}{n} \quad (5)$$

Moreover, the output voltage is derived as

$$V_O = V_I + V_{C3} + \left(\frac{1}{kn} + 1\right) V_{C2} \quad (6)$$

According to aforementioned assumption, the output capacitor voltage is constant during one switching period. Therefore, by equalization of (4) and (6), the following equation is derived as:

$$V_{C1} = \frac{kn+1}{kn} V_{C2} \quad (7)$$

Using the volt-second balance principle on Lm and equations (1), (3), (5) and (7), the voltages across capacitors C_1 and C_2 is obtained as

$$V_{C1} = \frac{(kn+1)D}{1-D} V_I \quad (8)$$

$$V_{C2} = \frac{knD}{1-D} V_I \quad (9)$$

Substituting (8) into (2), yields

$$V_{C3} = \frac{kn+1}{1-D} V_I \quad (10)$$

Substituting (9) and (10) into (6), the voltage gain is achieved as

$$M_{CCM} = \frac{2+kn+knD}{1-D} V_I \quad (11)$$

Fig.4 shows the variations of the voltage gain versus the duty ratio with different coupling coefficients of the coupled inductor. It can be seen that the coupling coefficient is not very effective on the voltage gain.

The voltage gain versus duty ratio of the proposed converter and the converters proposed under CCM operation with k = 1 and n = 2 are depicted in Fig.5. As it is shown n Fig. 5 the proposed converter has higher voltage transfer gain in comparison with other converters. Also, the voltage transfer gain of the presented converter is higher than the converter presented. However, in comparison with the presented converter, an additional diode, an extra capacitor, and a multi-winding coupled inductor is utilized in the converter.

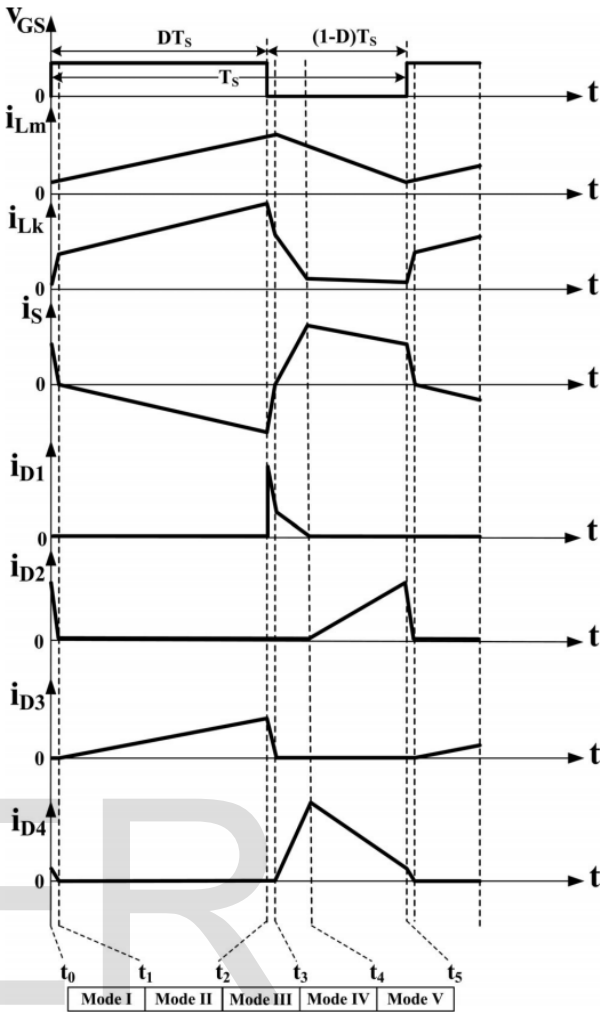

Fig.3. Some typical waveforms of the proposed converter at CCM operation.

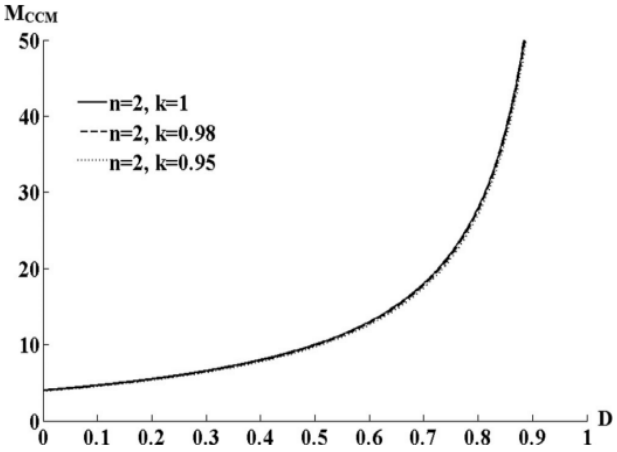

Fig.4. Voltage gain versus duty ratio under various coupling coefficients ofthe coupled inductor.

The voltage gain versus duty ratio of the proposed converter and the converters proposed under CCM operation with k = 1 and n = 2 are depicted in Fig.5. As it is shown n Fig. 5 the proposed converter has higher voltage transfer gain in comparison with other converters. Also, the voltage transfer gain of the presented converter is higher than

the converter presented. However, in comparison with the presented converter, an additional diode, an extra capacitor, and a multi-winding coupled inductor is utilized in the converter.

Based on the description of the operating modes, the voltage stresses on the active switch S and diodes D_1, D_2, D_3, and D_4 are expressed as

$$V_{DS} = V_{D1} = \frac{1}{1-D}V_I = \frac{1}{2+2n}(V_O + nV_I) \quad (13)$$

$$V_{D2} = \frac{n}{1-D}V_I = \frac{n}{2+2n}(V_O + nV_I) \quad (14)$$

$$V_{D3} = V_{D4} = \frac{1+n}{1-D}V_I = \frac{1}{2}(V_O + nV_I) \quad (15)$$

According to Fig.2, the average value of input current can be achieved as follows when switch is turned on/off:

$$I_{in(on)} = (n+1)I_{D3} + I_{L_m} \quad (16)$$

$$I_{in(off)} = I_O \quad (17)$$

From (16) and (17), the average current value of magnetizing inductor can be obtained as follows:

$$I_{L_m} = \frac{(M_{CCM} - 2 - n)I_O}{D} = \frac{2(n+1)}{1-D}I_O \quad (18)$$

The integral form of the current equation of magnetizing inductor can be written as

$$i_{L_m}(t) = i_{L_m}(t_0) + \frac{1}{L_m}\int_{t_0}^{t} v_{Lm}(\tau)d\tau \quad (19)$$

Substituting (16) into (19), and for k = 1, t = DT, and t_0 = 0, yields

$$\Delta i_{L_m} = \frac{DV_{in}}{L_m f_s} \quad (20)$$

According to Fig.3 and applying the ampere–second balance principle on capacitors, the average current values of diodes are equal to I_O. Therefore, the peak values of diodes D3 and D4 can be obtained as

$$i_{D3(peak)} = \frac{2I_O}{D} \quad (21)$$

$$i_{D4(peak)} = \frac{2I_O}{1-D} \quad (22)$$

$$i_{S(peak)} = i_{D1(peak)} = \left(\frac{2+n+nD}{D(1-D)}\right)I_O + \frac{DV_{in}}{L_m f_S} \quad (23)$$

Neglecting modes I and III, the time interval of modes IV and V are given as

$$d_4 = \frac{2I_O}{i_{D1(peak)}} = \frac{1-D}{n+1} \quad (24)$$

$$1 - D - d_4 = d_5 \quad (25)$$

From equation (25), the peak value of diode D_2 is obtained as

$$i_{D2(peak)} = \frac{2(n+1)I_O}{n(1-D)} \quad (26)$$

B. Boundary Conduction mode (BCM) Operation

Similar to the analysis done in the former section, the voltage conversion ratio of the presented converter in discontinuous conduction mode (DCM) can be obtained as follows:

$$M_{DCM} = \frac{V_O}{V_I} = \frac{n+2+\sqrt{(n+2)^2 + \frac{D^2}{\tau_{L_m}}}}{2} \quad (27)$$

If the proposed converter is operated in BCM, the voltage gain in the CCM will be equal to its voltage gain in the DCM operation. From (12) and (27), the boundary normalized magnetizing inductor time constant τLmB can be formulated as

$$\tau_{L_m,B} = \frac{D(1-D)^2}{8(n^2(1+D) + n(3+D) + 1)} \quad (28)$$

The normalized magnetizing-inductor time constant τ_{Lm} can be written as

$$\tau_{L_m} = \frac{f_s L_m}{R_L} \quad (29)$$

Fig.6 shows the curve of τ_{LmB}. If τ_{Lm} is larger than τLmB, the proposed converter is operated under CCM. Fig.7 shows the comparison of τ_{LmB} of the presented converter with converters with respect to the duty cycle and the conversion ratio. As it is shown in Fig.7, the CCM region of the presented converter is wider. Also, the CCM region of the presented converter is wider than the converter presented. Therefore, the presented converter requires a smaller magnetizing inductance to assure the CCM operation of the converter.

4. PROPOSED CONCEPT

A motor is an electrical machine which converts electrical energy into mechanical energy. The principle of working of a DC motor is that "whenever a current carrying conductor is placed in a magnetic field, it experiences a mechanical force". The direction of this force is given by Fleming's left hand rule and its magnitude is given by F = BIL. Where, B = magnetic flux density, I = current and L = length of the conductor within the magnetic field.

Fleming's left hand rule: If we stretch the first finger, second finger and thumb of our left hand to be perpendicular to each other AND direction of magnetic field is represented by the first finger, direction of the current is represented by second finger then the thumb represents the direction of the force experienced by the current carrying conductor.

When armature windings are connected to a DC supply, current sets up in the winding. Magnetic field may be provided by field winding (electromagnetism) or by using permanent magnets. In this case, current carrying armature conductors experience force due to the magnetic field, according to the principle stated above.

Commutator is made segmented to achieve unidirectional torque. Otherwise, the direction of force would have reversed every time when the direction of movement of conductor is reversed the magnetic field.

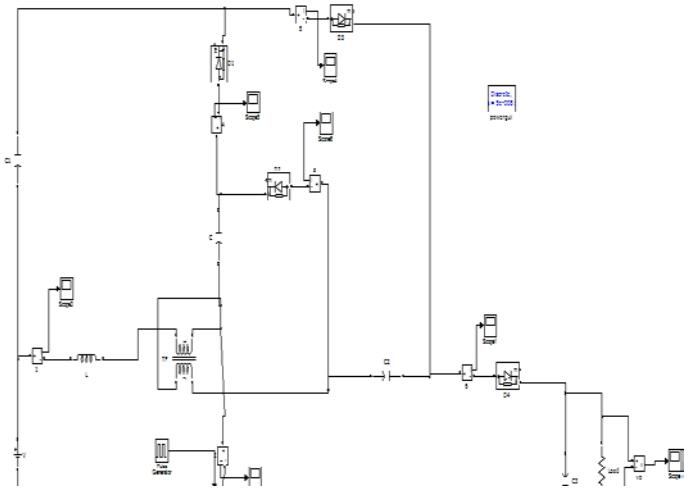

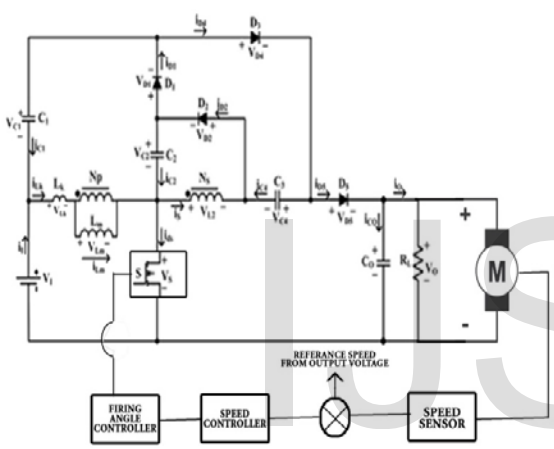

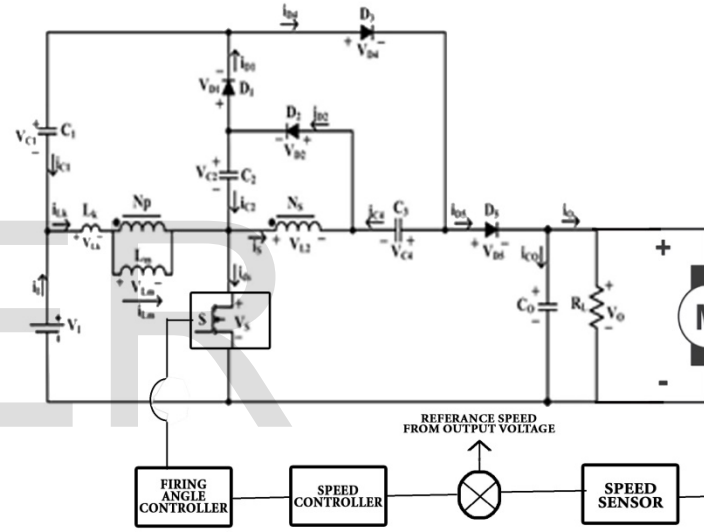

Fig.5.Circuit diagram of High Step-Up dc-dc converter with closed loop control of DC motor

A. Back EMF

According to fundamental laws of nature, no energy conversion is possible until there is something to oppose the conversion. In case of generators this opposition is provided by magnetic drag, but in case of dc motors there is back emf.

When the armature of the motor is rotating, the conductors are also cutting the magnetic flux lines and hence according to the Faraday's law of electromagnetic induction, an emf induces in the armature conductors. The direction of this induced emf is such that it opposes the armature current (I_a). The circuit diagram below illustrates the **direction of the back** emf and armature current. Magnitude of **Back emf** can be given by the emf equation of DC generator.

Fig.7 Diode (D_1) Current

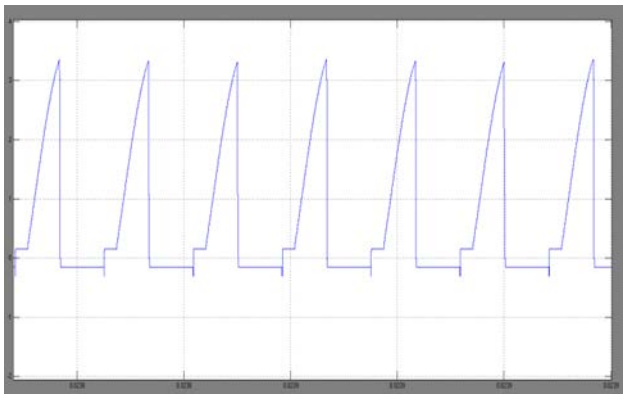

Fig.8 Diode (D_2) Current

5. MATLAB/SIMULINK RESULTS

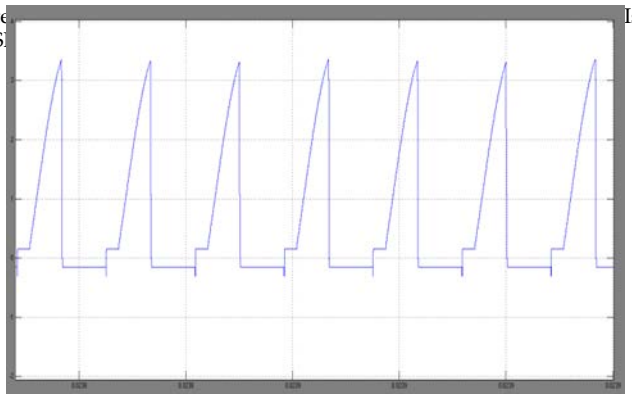

Fig.8 Diode (D_2) Current

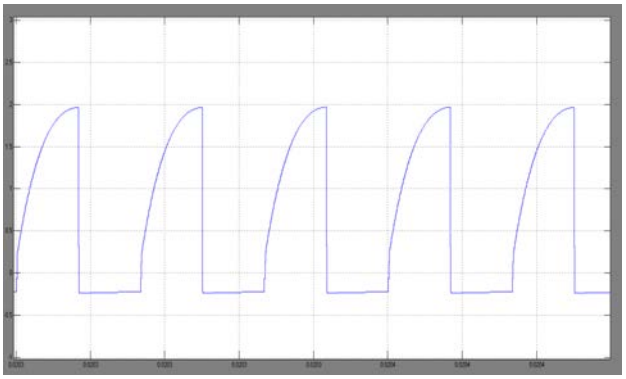

Fig.9 Diode (D_3) Current

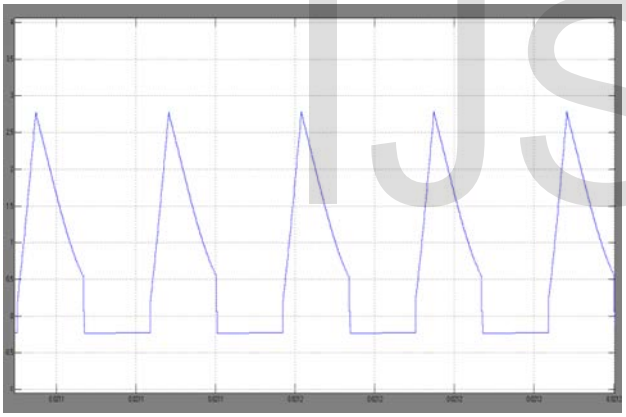

Fig.10 Diode (D_4) Current

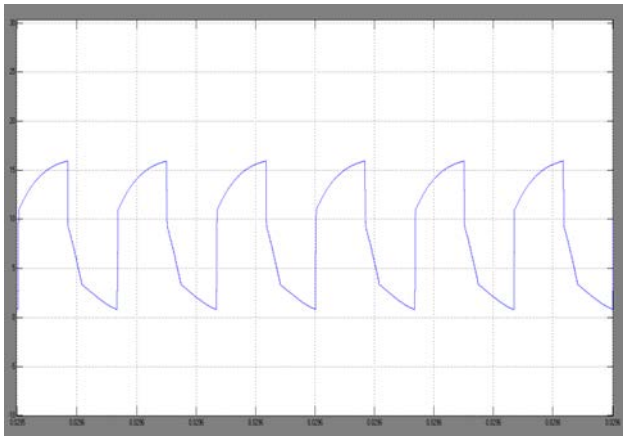

Fig.11 Inductor Current

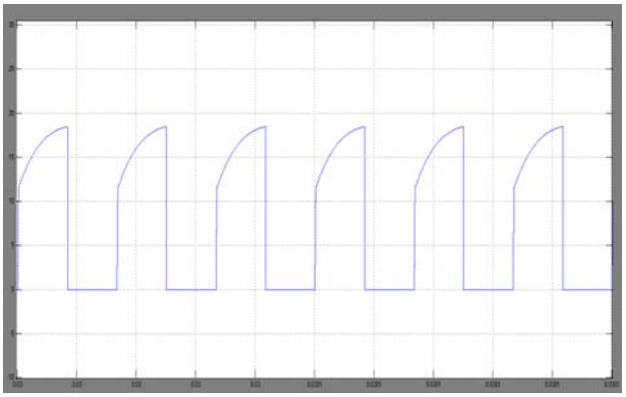

Fig.12 Switch Current

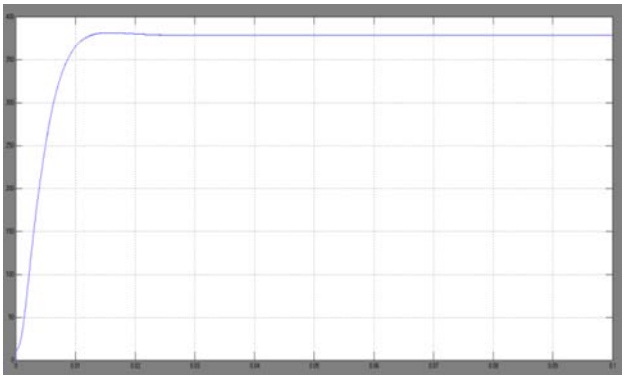

Fig.13 Output Voltage

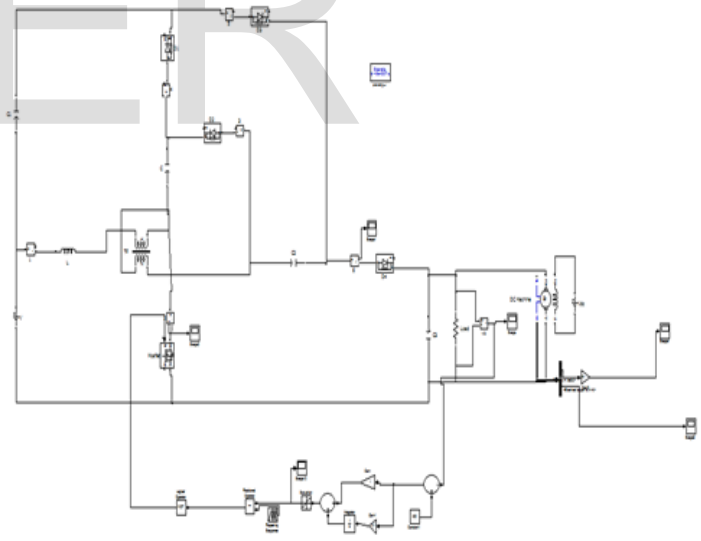

Fig.14 Matlab/Simulink model of High Step-Up dc-dc converter with closed loop control of DC motor

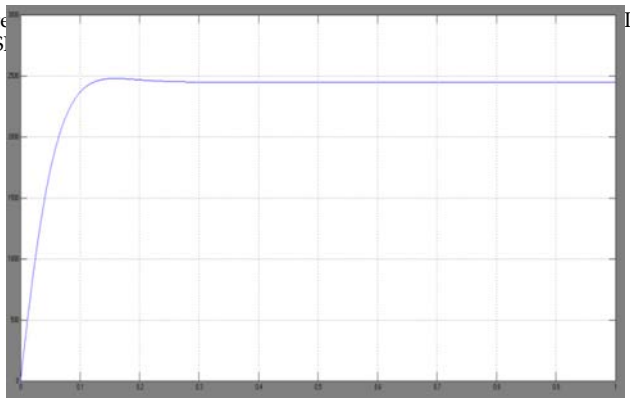

Fig.15 Speed of the DC motor

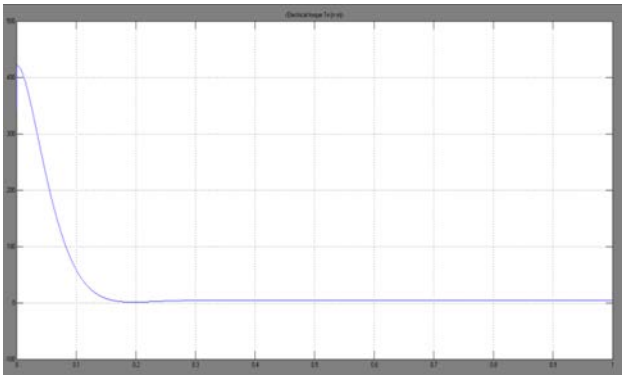

Fig.16 Torque characteristics of the DC motor

6. CONCLUSION

A high step-up dc/dc converter based on integrating coupled inductor and switched-capacitor are proposed for renewable energy applications. The energy stored in the leakage inductance of the coupled inductor is recycled by using switched capacitors. The voltage stress across the main switch is reduced. Here the gate signals are generated using PWM control schemes. The suggested converter is suitable for DC Motor based energy sources, which require high-step-up voltage transfer gain. The proposed concept is implemented with Dc motor operating in closed loop operation using Matlab/simulink software.

REFERENCES

Statements that serve as captions for the entire table do not need footnote letters.

[5] C. Olalla, C. Deline and, and D. Maksimovic, "Performance of mismatched PV systems with submodule integrated converters," IEEE J. Photovoltaic, vol. 4, no. 1, pp. 396–404, Jan. 2014.

[6] C. W. Chen, K. H. Chen, and Y. M. Chen, "Modeling and controller design of an autonomous PV module for DMPPT PV systems," IEEE Trans. Power Electron., vol. 29, no. 9, pp. 4723–4732, Sep. 2014.

[7] Y. P. Hsieh, J. F. Chen, T. J. Liang, and L. S. Yang, "Analysis and implementation of a novel single-switch high step-up DC–DC converter," IET Power Electron., vol. 5, no. 1, pp. 11–21, Jan. 2012.

[8] Y. Zhao, W. Li, Y. Deng, and X. He, "High step-up boost converter with passive lossless clamp circuit for non-isolated high step-up applications," IET Power Electron., vol. 4, no. 8, pp. 851–859, Sep. 2011.

[9] I. Laird and D. D. Lu, "High step-up DC/DC topology and MPPT algorithm for use with a thermoelectric generator," IEEE Trans. Power Electron., vol. 28, no. 7, pp. 3147–3157, Jul. 2013.

[10] R. J. Wai, C. Y. Lin, C. Y. Lin, R. Y. Duan, and Y. R. Chang, "Higheffi-ciency power conversion system for kilowatt-level stand-alone generation unit with low input voltage," IEEE Trans. Ind. Electron., vol. 55, no. 10, pp. 3702–3714, Oct. 2008.

[11] L. S. Yang, T. J. Liang, and J. F. Chen, "Transformer-less DC–DC converter with high voltage gain," IEEE Trans. Ind. Electron., vol. 56, no. 8, pp. 3144–3152, Aug. 2009.

[12] Y. P. Hsieh, J. F. Chen, T. J. Liang, and L. S. Yang, "Novel high step-up DC–DC converter with coupled-inductor and switched-capacitor techniques," IEEE Trans. Ind. Electron., vol. 59, no. 2, pp. 998–1007, Feb. 2012.

[13] J. A. Carr, D. Hotz, J. C. Balda, H. A. Mantooth, A. Ong, and A. Agarwal, "Assessing the impact of SiC MOSFETs on converter interfaces for distributed energy resources," IEEE Trans. Power